frontiers

Revisiting the δ Scuti Star FG Virginis using *Kepler K2* and *TESS* data

Joyce A. Guzik[1*], Jason Jackiewicz[2], Anne M. Hedlund[1,2]

[1]Los Alamos National Laboratory, Los Alamos, NM 87545, USA
[2]Department of Astronomy, New Mexico State University, Las Cruces, NM 88003, USA

*** Correspondence:**
Joyce A. Guzik
joy@lanl.gov

Keywords: stars: pulsations, stars: evolution, asteroseismology, stars: δ Scuti, stars: FG Vir, NASA *Kepler* mission, NASA *TESS* mission, NASA *K2* mission

Abstract

FG Virginis is a δ Scuti variable star that was the target of several ground-based multisite photometric campaigns from 1992 to 2004. Over 75 pulsation frequencies were detected (Breger et al. 2005), more than for any other δ Sct star before the era of space photometry. FG Vir was observed for 52 days in 30-minute cadence photometry by the NASA *Kepler* spacecraft *K2* mission in 2016, and for 23 days in 2-minute cadence photometry by the NASA *TESS* spacecraft in 2021. We present light curves and amplitude spectra obtained from these space missions. We find around 40 significant frequencies in the *K2* data, and at least 100 significant frequencies in a first look at the *TESS* data. There is good correspondence between the first 10 or so highest-amplitude modes found in the *K2* and *TESS* data and those found from the ground-based multisite campaigns, although the amplitude order is slightly different, indicating some stability in mode frequencies and amplitudes spanning 20 years. However, the 9th highest-amplitude mode of Breger et al. has moved down considerably in amplitude rank, while the 35th highest-amplitude mode has moved up to near the top ten as seen in both the *K2* and *TESS* data. We find several low frequencies between 0.3 and 3 cycles per day in the TESS data that were not detected using the ground-based data. If low frequency pulsations are confirmed, FG Vir would be classified as a δ Sct/γ Dor hybrid variable star. We also review stellar model results and some of the challenges for asteroseismology for this well-studied δ Sct star.

1 Introduction

The δ Scuti variables are main-sequence or slightly post-main sequence stars with mass around 2 $M_{\odot}$, which pulsate in one or more radial or non-radial modes (Aerts et al. 2010). These stars are of interest for asteroseismology, i.e., using the pulsation properties in conjunction with modeling to derive stellar interior structure and to test theories of stellar evolution and pulsation driving.

FG Virginis (HD 106384) is a well-studied bright (V = 6.558) δ Scuti star of spectral type A8. FG Vir was the object of ground-based single-site (1982; see Lopez de Coca et al. 1984) and multisite (1992-2004; see Breger et al. 1995, 1996, 1998, 2004, 2005, Breger and Lenz 2019) photometric campaigns. These campaigns resulted in detection of 75+ pulsation frequencies (Breger et al. 2005), more than any other δ Sct star before the era of long time-series space photometric missions such as CoRoT (Poretti et al. 2009), *Kepler* (Borucki et al. 2010, Gilliland et al. 2010, Koch et al. 2010), and *TESS* (Riker et al. 2015). See also Guzik (2021) and Daszynska-Daszkiewicz et al. (2005, 2021) for more information about δ Sct stars and results from space missions.

FG Vir was observed for 52.5 days in 30-minute cadence photometry by the NASA *Kepler* spacecraft during Campaign 10 (6 July – 20 Sept. 2016) of the extended *Kepler* mission (*K2*, Howell et al. 2014) as part of our request to the Guest Observer program (see Guzik et al. 2019). FG Vir was observed by the NASA TESS spacecraft for 23 days in Dec. 2021. We present a first look at the amplitude spectra derived from these data, and comparisons with the amplitude spectra obtained using the ground-based multisite data. We also review some of the findings from asteroseismology and unanswered questions for this interesting δ Sct star.

2 *Kepler* Data Analysis and Results

FG Vir is EPIC 201132898 in the *K2* Ecliptic Plane Input Catalog (Huber et al. 2016). We retrieved the pre-search data conditioning simple-aperture photometry (PDC_SAP) light-curve data from the Mikulski Archive for Space Telescopes (MAST, https://archive.stsci.edu/). Figure 1 shows the *K2* light curve and a 3-day zoom-in on a portion of the light curve. Figure 2 shows the amplitude spectrum resulting from a Fourier analysis of the light curve and a zoom-in on the lower-amplitude frequencies. To determine the significant frequencies, the highest-amplitude modes were removed from the light curve successively until only noise remained, a process called pre-whitening. For evenly spaced 30-min cadence data, the Nyquist frequency limit is 24.4695 c/d, so the amplitude spectrum is truncated at this frequency.

Table 1 lists the 46 frequencies obtained from the pre-whitening analysis in order of signal-to-noise ratio (S/N), down to S/N ~ 3. Table 1 also notes associations of these frequencies with those from Breger et al. (2005) obtained using multisite observations. Considering the first 11 modes, apart from two modes with very close frequency to the highest-amplitude mode, all of them are found among the 10 highest-amplitude modes of Breger et al., although the amplitude ordering is slightly different. Breger et al.'s 9th highest-amplitude mode (frequency 19.228 c/d) is only the 19th highest-amplitude using the *K2* data. Some of the remaining modes found from the *K2* data can be associated with the Breger et al. frequencies. It is interesting that the 35th highest-amplitude mode in the Breger et al. list (frequency 20.511 c/d) corresponds to the 13th highest in the *K2* data.

The three lowest-frequency *K2* modes can be associated with multiples of close frequency differences between high-amplitude modes f1, f2, and f9. To compensate for the loss of a second reaction wheel, the *K2* mission used solar radiation pressure to keep the spacecraft pointed in the same direction, and in addition fired thrusters every 5.8849 hours (*K2* Handbook, Mighell and Van Cleve 2020). The thruster-firing frequency of 4.0782 c/d and its 2nd harmonic at 8.1564 c/d appear in the *K2* frequency list. Two other low-frequency modes at 0.47434 and 0.49454 c/d are combinations of the f2 and f9 modes minus 3x the thruster-firing frequency.

Apart from these combinations, there remain 11 modes, highlighted in red font in Table 1, with frequencies 0.3 to ~3 c/d, in the right frequency range to be γ Dor gravity modes (see, e.g., Aerts et al. 2010). Most of these are among the lowest-amplitude modes, and seven have S/N < 3.5, so are likely to be spurious. However, if low-frequency modes were to be detected, FG Vir would be considered a hybrid δ Sct/γ Dor variable-star candidate.

We truncate the *K2* frequency search at the Nyquist limit of 24.4691 c/d for evenly spaced 30-min cadence data. The multisite data is not evenly spaced, and Breger et al. (2005) find frequencies up to 44.2591 c/d. One *K2* frequency at 14.36915 c/d may be a Nyquist-reflected frequency, associated with the 34.5737 f23 mode of the Breger et al. list.

3 Preliminary Look at *TESS* Data

The *Kepler* spacecraft was retired in November 2018; the *TESS* spacecraft (Riker et al. 2015) was launched in April 2018 into a 13.7-day elliptical orbit around Earth, maintained by a 2:1 lunar resonance. *TESS* data for FG Vir is now available at MAST, taken during the 27.4 observing days of sector 46 (Dec. 2-30, 2021). Moreover, data were taken at 2-minute cadence, so the S/N is much larger and Nyquist frequency limit much higher than for the 30-min cadence *K2* data.

FG Vir is TIC 277227048 in the *TESS* Input Catalog (Stassun et al. 2019). Figure 3 (left) shows the *TESS* FG Vir light curve, including data from 22.84 days, excluding the gap of about 5 days in the middle of the data set. Figure 3 (right) shows a 1-day zoom-in on the light curve; small features are resolved in the *TESS* 2-min cadence light curve that were not resolvable in *K2* 30-min cadence light curve.

Figure 4 shows the FG Vir amplitude spectrum using *TESS* data, truncated at 50 c/d, and also a zoom-in at lower amplitudes. We performed pre-whitening analysis for the first 100 modes with the highest S/N ratios. The S/N of the 100th peak is 27, so it is likely that many more significant frequencies remain in the residual.

Table 2 lists these 100 frequencies in order of amplitude, and notes associations with Breger et al. (2005) frequencies. No significant frequencies were apparent at frequencies > 50 c/d. The 9 highest-amplitude *TESS* frequencies are found among the 10 highest-amplitude Breger et al. (2005) frequencies, although the amplitude order is slightly different. The 9th highest-amplitude frequency in the Breger et al. list is 29th in the *TESS* data, while f35 in the Breger et al. list is 10th highest in the *TESS* data, confirming the significant amplitude changes in these modes found using the *K2* data.

Table 2 includes four low frequencies between 0.3 and 3 c/d, highlighted in red font. These frequencies are more likely to be real, as opposed to the low frequencies in the *K2* data, as their signal-to-noise ratio is high. These low frequencies do not coincide with any of the likely spurious low frequencies found in the *K2* data. If confirmed as gravity mode pulsations, FG Vir would be classified as a δ Sct/γ Dor hybrid.

4 Unresolved Questions for Asteroseismology

As discussed by, e.g., Guzik (2021), there are many inter-related unresolved problems for δ Sct stars that make asteroseismology challenging.

First, there is a mode visibility problem for non-radial oscillations as seen in δ Sct stars. Temperature variations described by spherical harmonic patterns average out over the unresolved stellar disk, making higher degree (ℓ) modes more difficult to see in photometry. Usually, it is expected to detect modes of degree 0 (radial), 1 (dipole), and 2 (quadrupole). Is it possible to measure modes of degree ℓ = 3 or higher, particularly with the higher precision and longer continuous time series possible with space-based photometry? Daszynska-Daszkiewicz et al. (2006) conclude that modes of degree ℓ = 3 and probably much larger ℓ should be visible, even using the FG Vir ground-based data, and that most of the modes discovered for FG Vir below 30 c/d must have ℓ > 2!

Second is the rotational splitting problem. Stellar rotation splits modes into $2\ell + 1$ separate multiplets, and rotation can shift frequencies even for radial (ℓ =0) modes. FG Vir's equatorial rotation velocity is 30-80 km/sec (Mantegazza and Poretti 2002, Zima et al. 2006), so we should expect a rotational

splitting frequency of around 0.5 c/d for FG Vir stellar radius ~2.2 $R_\odot$. We don't see obvious rotationally split modes in the FG Vir amplitude spectrum.

Third is the mode selection problem. Not all of the modes expected from stellar models for δ Sct stars are seen in the amplitude spectrum. Also, there are modes observed that are not expected from the best-fit pulsation models.

Then there is the mystery of amplitude and frequency variations, found in many types of variable stars, including δ Sct stars (see, e.g., Bowman et al. 2016). Amplitudes and frequencies of individual δ Sct modes can be relatively stable over time. It is possible to associate many of the highest-amplitude modes in the *K2* (2016) and *TESS* (2021) data sets with modes in the Breger et al. (2005) list. However, the order of the mode amplitudes is somewhat different for the first dozen or more modes; some modes appear in the *K2* and *TESS* data that aren't in the Breger et al. list, and vice versa; and the Breger et al. f9 mode has moved down in amplitude rank, while the f35 mode increased in rank. Nonlinear mode-coupling effects are suspected as the cause of these variations.

Breger and Pamyatnykh (2006) investigate the problem of closely spaced modes in FG Vir, with separations less than 0.1 c/d, too small to be the result of rotational splitting. Are these separate modes, or are they the result of amplitude variability of a single frequency? Breger and Pamyatnykh (2006) were able to rule out amplitude variability for several of the FG Vir closely spaced modes.

These many complications lead to a mode identification problem. We can't identify modes by patterns in the amplitude spectrum and match them directly with modes expected from theoretical models. However, methods have been developed to identify the angular degree (ℓ) and azimuthal order (m) of the highest-amplitude modes using color photometry, phase information, line profile variations and radial velocities from spectroscopy (see, e.g., Breger et al. 1999, Mantegazza and Poretti 2002, Daszynska-Daszkiewicz et al. 2005, Zima et al. 2006, Viskum et al. 2008). Some FG Vir modes have been identified using these methods, but mode identification has been somewhat uncertain. For example, Daszynska-Daszkiewicz et al. (2005) identified the angular degrees for twelve FG Vir modes to 80% probability, but there are ambiguities for six of these modes. In early studies of FG Vir, the highest-amplitude mode at 12.7162 c/d was thought to be the radial fundamental mode (e.g., Mantegazza et al. 1994, Breger et al. 1995), but later studies (e.g., Viskum et al. 1998, Mantegazza and Poretti 2002) showed that this mode is most likely an ℓ=1 dipole mode, and the radial fundamental mode is actually the 2nd highest-amplitude mode at 12.1541 c/d.

Attempts have been successful to find patterns of frequency spacings (e.g., Breger, et al 2009). The spacings could correspond to the large separations between modes of successive ℓ values, or a rotational splitting spacing, or a combination of these two spacings (see also Paparo et al. 2016a,b, Suarez et al. 2014, Bedding et al. 2020). Patterns of mode spacings can therefore be useful to identify modes of common ℓ value, determine the stellar mean density, or even to measure the stellar interior rotation rate.

5 FG Vir Models

The goal of asteroseismology of FG Vir is to use the observed frequency properties to determine the stellar interior structure and evolution state. Evolution and pulsation models of FG Vir have been calculated over the years to attempt to make use of the observed frequencies. It is helpful to have additional constraints from multicolor photometry, spectroscopy, and stellar model grids to provide a starting point for detailed model explorations. The *TESS* Input Catalog (TIC, Stassun et al. 2019) lists

FG Vir properties collected from several sources: effective temperature T_{eff} = 7361 ± 131 K, log surface gravity (log g) = 3.974 ± 0.086, radius R = 2.205 ± 0.082 $R_\odot$, mass M = 1.6 ± 0.282 $M_\odot$, luminosity L=12.86 ± 0.44 $L_\odot$, and distance 83.02 ± 0.37 pc.

Viskum et al. (1998) use FG Vir frequencies to derive a mean stellar density (ρ) = 0.1645 ± 0.005 $\rho_\odot$. Assuming T_{eff} = 7500 K and metallicity Z = 0.02, they find M = 1.82 ± 0.03 $M_\odot$, L = 14.1 ± 0.9 $L_\odot$, R = 2.227 ± 0.012 $R_\odot$, and log g = 4.002 ± 0.003. Their derived luminosity places FG Vir at a distance of 82 ± 3 pc.

Breger et al. (1999) find a best-fit model to the FG Vir frequencies with M = 1.95 $M_\odot$, T_{eff} = 7492 K, L = 14.92 $L_\odot$, R = 2.301 $R_\odot$, and log g = 4.002. This model has metallicity Z=0.02, initial helium mass fraction Y = 0.28, and mean density 0.1597 $\rho_\odot$. The model uses artificially modified opacities, and core convective overshooting.

Templeton et al. (2001) find a best-fit model for FG Vir with M = 1.9 $M_\odot$, T_{eff} = 7413 K, L = 14.16 $L_\odot$, and age 0.93 Gyr. This model has Z=0.03 and hydrogen mass fraction Y=0.28, and it includes core convective overshooting.

Kirbiyik et al. (2004) evolve models with uniform rotation and conservation of angular momentum, and calculate pulsation frequencies including first-order rotational splitting. Their paper does not discuss whether convective overshooting is included. They find best-fit models for FG Vir with M = 1.85 $M_\odot$, T_{eff} = 7540-7560 K, L =15.06-15.12 $L_\odot$ and rotation rate 32-66 km/s.

Table 3 lists the ℓ = 0, 1, 2, and 3 pulsationally unstable frequencies for an FG Vir model calculated by Guzik. These model frequencies were used by Paparo et al. (2016a,b) to illustrate how frequency spacings could be used to help identify modes in δ Scuti stars. The physics of the models is the same as used in the Guzik et al. (2000) FG Vir models. The model does not include core convective overshooting. A model was selected on the 1.82 $M_\odot$, Z=0.02, Y=0.28 evolutionary track that has radial fundamental mode frequency 12.1541 c/d, identified as the FG Vir radial fundamental mode. For this model, L = 13.92 $L_\odot$, T_{eff} = 7419 K, R = 2.26 $R_\odot$, log g = 3.9896, and mean density 0.1577 $\rho_\odot$. The model age is 0.867 Gyr, and core helium mass fraction is 0.708, indicating that about 2/3 of the core hydrogen has been converted to helium.

The calculated model frequencies in Table 3 do not include rotational splitting, which will divide non-radial modes into 2 ℓ + 1 multiplets, with spacings of around 0.5 c/d, depending on the rotational velocity adopted. A total of 98 ℓ =0, 1, and 2 modes are predicted, taking into account rotational splitting. However, even including rotational splitting, not all of the observed frequencies of Breger et al. (2005) can be matched for FG Vir. Considering in addition the 15 calculated unstable ℓ =3 modes would increase the total number of predicted modes by another 105, to 203. As discussed in Section 4, it is possible that modes of even higher angular degree are visible in photometric data.

In summary, the stellar properties derived for FG Vir using asteroseismic data and stellar models are in good agreement with each other and also consistent with properties derived from spectroscopy and the distance derived from parallax measurements. However, none of the models to date provide an exact fit to all of the observed FG Vir frequencies, and there is much more that could be learned about FG Vir's evolution and interior structure using these data.

It is an interesting question whether FG Vir has a stellar or planetary companion, and whether these objects might affect pulsation properties. FG Vir is listed as a visual binary in the catalog of Liakos and Niarchos (2017), who reference catalogs of Abt (1981) and Mason et al. (2001). However, the properties of the binary companion and orbital period are not given in these catalogs. An angular separation of 0.1 arc sec is given by Mason et al., but this separation may be a lower limit to the resolution of the observations.

Kervella et al. (2019) use Hipparcos (van Leeuwen 2007) and Gaia DR2 (Gaia Collaboration 2016, 2018) data to discover stellar and substellar companions using proper motion anomalies. They find a proper motion anomaly of 3.89 σ using Hipparcos data, and an anomaly at only the 1.37 σ level using Gaia DR2 data. Assuming the Gaia DR2 proper-motion anomaly is real, they estimate a 4.27 Jupiter-mass companion, normalized to distance 1 A.U.

6 Conclusions

We compare the FG Vir frequencies detected using 52.4 days of 30-min cadence *Kepler K2* photometry with those detected using at least 363 nights (Breger and Lenz 2019) of multisite ground-based network data. More than 75 significant frequencies were measured in the ground-based data (Breger et al. 2005), compared to around 40, depending on S/N limit adopted, using the *K2* data. The *K2* frequency detections were limited to frequencies below the Nyquist frequency limit of ~24.5 c/d for 30-min equally spaced data, while frequencies as high as 44.25 c/d were identified using the ground-based data. The ground-based multisite data included color photometry, which turned out to be extremely useful for mode identifications of the highest-amplitude modes.

The *TESS* data appear more promising for further FG Vir discoveries. The time-series length of the *TESS* data was 22.84 days, shorter than for the *K2* series, but the shorter 2-minute cadence increased greatly the S/N, allowing the detection of at least 100 modes with S/N > 27. The 2-minute cadence also increased the Nyquist frequency limit, so that modes up to 45 c/d, as found in the ground-based data, were detected. The *TESS* data should reveal many more modes of even lower amplitude than found in the ground-based data, requiring consideration of modes of angular degree $\ell > 3$ for asteroseismic models. The increased number of detected modes will make mode identification even more challenging!

There is general agreement among the frequencies of the 10 highest-amplitude modes between the ground-based, *K2*, and *TESS* data. Two modes of interest are the f9 mode of Breger et al. (2005), which moved down in amplitude rank, and the f35 mode of Breger et al., which moved up in amplitude rank according to both the *K2* and *TESS* data.

The continuity of the *K2* and *TESS* data, and, possibly, the elimination of day/night aliases, enables detection of low-frequency modes. Several modes of significant amplitudes with frequencies between 0.3 and 3 c/d were detected in the TESS data, which may be high-order γ Dor gravity-mode pulsations. If confirmed, FG Vir would be a hybrid δ Sct/γ Dor variable star.

7 Author Contributions

J.G. wrote the text of this article, created the figures and tables, and calculated the FG Vir model discussed. J.J. performed the analysis of the FG Vir *Kepler* and *TESS* data, including processing light curves, performing the pre-whitening analysis to identify significant frequencies, identifying

combination frequencies. A.H. contributed by reviewing literature on possible FG Vir binary companions.

8 Funding

We acknowledge a Los Alamos National Laboratory Center for Space and Earth Sciences grant CSES XX8P. J.G. acknowledges support from LANL, managed by Triad National Security, LLC for the U.S. DOE's NNSA, Contract #89233218CNA000001.

9 Acknowledgments

We are grateful for data from the NASA *Kepler* and *TESS* spacecraft, and the opportunities to propose these observations via the *K2* Guest Observer and *TESS* Guest Investigator programs. This research has made use of the SIMBAD database, operated at CDS, Strasbourg, France, and the Mikulski Archive for Space Telescopes (MAST). J.G. thanks the Society for Astronomical Sciences for the opportunity to present these results at their 2022 Symposium for Telescope Sciences.

10 References

Abt, H., Visual multiples. VII. MK classifications, ApJ Suppl. Ser. 45, 437 (1981).

Aerts, C., Christensen-Dalsgaard, J., and Kurtz, D.W., Asteroseismology, Springer Astronomy & Astrophysics Library (2010).

Bedding, T., et al., Very regular high-frequency pulsation modes in young intermediate-mass stars, Nature Vol. 581, doi.org/10.1038/s41586-020-2226-8 (2020).

Borucki, W.J., et al., *Kepler* planet-detection mission: Introduction and First Results, Science 327, 9777 (2010).

Bowman, D.M., et al., Amplitude modulation in δ Sct stars: statistics from an ensemble study of *Kepler* targets, MNRAS 460, 1970 (2016).

Breger, M. and Lenz, P., Photometric data by the δ Scuti Network II. EE Cam, FG Vir, 44 Tau, The Journal of Astronomical Data 25, 1 (2019).

Breger, M. and Pamyatnykh, A.A., Amplitude variability or close frequencies in pulsating stars—the δ Scuti star FG Vir, MNRAS 368, 571 (2006).

Breger, M., et al., The δ Scuti star FG Virginis. I. Multiple pulsation frequencies determined with a combined DSN/WET campaign, A&A 297, 473 (1995).

Breger, M., et al., The δ Scuti star FG Virginis. II. A search for high pulsation frequencies, A&A 309, 197 (1996).

Breger, M., et al., The δ Scuti star FG Vir. III. The 1995 multisite campaign and the detection of 24 pulsation frequencies, A&A 331, 271 (1998).

Breger, M., et al., The δ Scuti star FG Vir. IV. Mode identification and pulsation modelling, A&A 341, 151 (1999).

Breger, M., et al., The δ Scuti star FG Vir. V. The 2002 photometric multisite campaign, A&A 419, 695 (2004).

Breger, M. et al., Detection of 75+ pulsation frequencies in the δ Scuti star FG Virginis, A&A 435, 955 (2005).

Breger, M., Lenz, P., and Pamyatnykh, A.A., Towards mode selection in δ Scuti stars: regularities in observed and theoretical frequency spectra, MNRAS 396, 201 (2009).

Daszynska-Daszkiewicz, J., Dziembowski, W.A., and Pamyatnykh, A.A., Mem. S.A.It. 77, 113 (2006).

Daszynska-Daszkiewicz, J., et al., Inferences from pulsational amplitudes and phases for multimode δ star FG Vir, A&A 438, 653 (2005).

Daszynska-Daszkiewicz, J., et al., Mode identification and seismic study of δ Scuti, the prototype of a class of pulsating stars, MNRAS 505, 88 (2021).

Gaia Collaboration, Prusti, T., et al., The Gaia Mission, A&A 595, A1 (2016).].

Gaia Collaboration, Brown, A.G.A., et al. Gaia Data Release 2. Summary of the contents and survey properties, A&A 616, A1 (2018).

Gilliland, R.L., et al., *Kepler* Asteroseismology Program: Introduction and First Results, PASP 122, 131 (2010).

Guzik, J.A., Bradley, P.A., and Templeton, M.R., Approaches to Asteroseismology of Core and Shell Hydrogen-Burning δ Scuti Stars, in δ *Scuti and Related Stars*, ASP Conference Series Vol. 210, 2000, eds. M. Breger and M.H. Montgomery.

Guzik, J.A, Garcia, J., and Jackiewicz, J., Properties of 249 δ Scuti Variable Star Candidates Observed During the NASA *K2* Mission, Frontiers in Astronomy and Space Sciences, doi: 10.3389/fspas.2019.00040 (2019).

Guzik, J.A., Highlights of discoveries for δ Scuti variable stars from the *Kepler* Era, Frontiers in Astronomy and Space Sciences, doi: 10.3389/fs-pas.2021.653558 (2021).

Howell, S.G., et al., The *K2* Mission: Characterization and Early Results, PASP 126, 398 (2014).

Huber, D., et al., The *K2* Ecliptic Plane Input Catalog (EPIC) and Stellar Classifications of 138,600 Targets in Campaigns 1–8, ApJ Suppl. Ser. 224, 2 (2016).

Kervella, P., et al., Stellar and substellar companions of nearby stars from Gaia DR2: Binarity from proper motion anomaly, A&A 623, 72 (2019).

Kirbiyik, H., et al., A new oscillating model suggestion for FG Vir, Astrophys. Space Sci. 295, 473 (2004).

Koch, D.G., et al., *Kepler* Mission Design, Realized Photometric Performance, and Early Science, ApJ Letters 713, L79 (2010).

Liakos, A., and Niarchos, P., Catalogue and properties of δ Scuti stars in binaries, MNRAS 465, 1181 (2017).

Lopez de Coca, P., Garrido, R., Costa, V., and Rolland, A., Narrow Band Photometry of FG Vir, Commission 27 of the I.A.U. Information Bulletin on Variable Stars, Number 2465, 27 January 1984.

Mantegazza, L., Poretti, E., and Bossi, M., Simultaneous intensive photometry and high-resolution spectroscopy of δ Scuti stars. I. Mode typing of HD 106384 = FG Virginis, A&A 287, 95 (1994).

Mantegazza, L. and Poretti, E., Line profile variations in the δ Scuti star FG Virginis: A high number of axisymmetric modes, A&A 396, 911 (2002).

Mason, B.D., et al., The 2001 US Naval Observatory Double Star CD-ROM. I. The Washington Double Star Catalog, AJ 122, 3466 (2001).

Mighell, K. and Van Cleve, J., *K2*, Extending *Kepler's* Power to the Ecliptic, *K2* Handbook, KSCI-19166-003, NASA Ames Research Center, Moffett Field, CA, 24 August 2020.

Paparo, M., et al., Unexpected series of regular frequency spacing of δ Scuti stars in the non-asymptotic regime. I. The Methodology, ApJ 822, 100 (2016a).

Paparo, M., et al., Unexpected series of regular frequency spacing of δ Scuti stars in the non-asymptotic regime. II. Sample-echelle diagrams and rotation, ApJ Supp. Ser. 224, 41 (2016b).

Poretti, E., et al., HD 50844: a new look at δ Scuti stars from CoRoT space photometry, A&A 506, No. 1, p. 85 (2009).

Riker, G.R., et al., Transiting Exoplanet Survey satellite (*TESS*), J. Astron. Telesc. Instr. Syst. 1:014003 (2015).

Stassun, K., et al., The Revised *TESS* Input Catalog and Candidate Target List, AJ 158, 138 (2019).

Suarez, J.C., Garcia Hernandez, A., and Moya, A., Measuring mean densities of Scuti stars with asteroseismology, A&A 563, A7 (2014).

Templeton, M., Basu, S., and Demarque, P., Asteroseismology of δ Scuti Stars: A Parameter Study and Application to Seismology of FG Virginis, ApJ 563, 999 (2001).

Van Leeuwen, F., Hipparcos, the New Reduction of the Raw Data, Astrophysics and Space Science Library, Volume 350, ISBN 978-1-4020-6341-1, Springer Science+Business Media B.V. (2007).

Viskum, M., et al., Oscillation mode identifications and models for the δ Scuti star FG Virginis, A&A 335, 549 (1998).

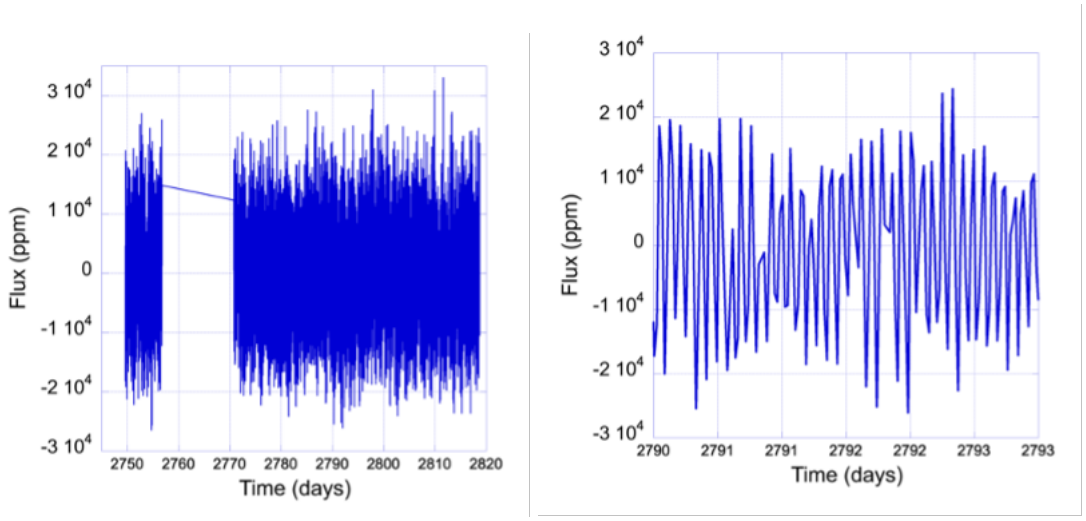

Figure 1. Left: FG Vir *K2* 30-min cadence light curve from Campaign 10, showing 52.5 days of data, excluding the gap near the beginning of the data set. Time is measured after barycentric Julian day 2454833.0. Right: 3-day zoom-in on FG Vir *K2* light curve.

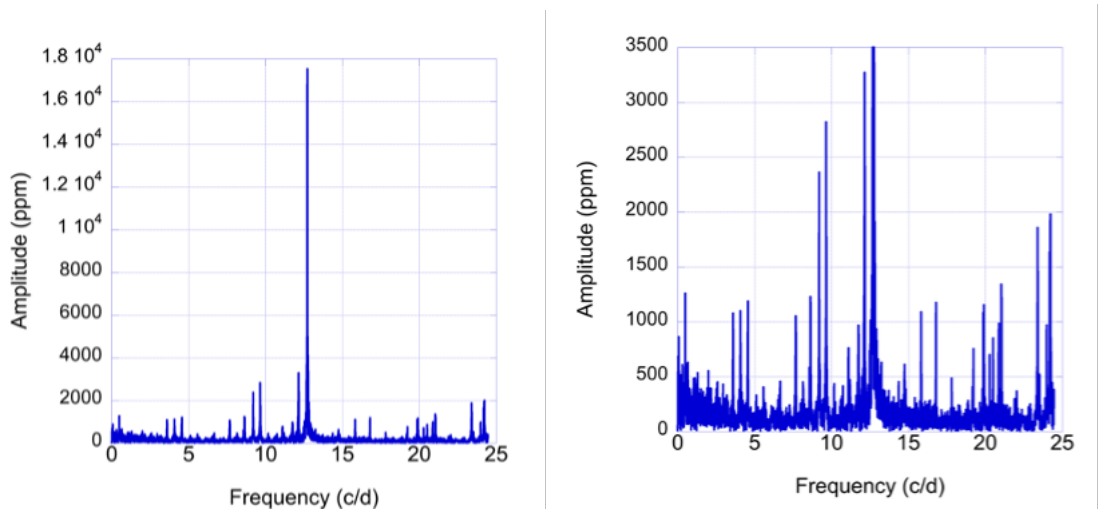

Figure 2. Left: FG Vir *K2* amplitude spectrum from 0 to 24.5 c/d. Right: Zoom-in on low-amplitude region of amplitude spectrum.

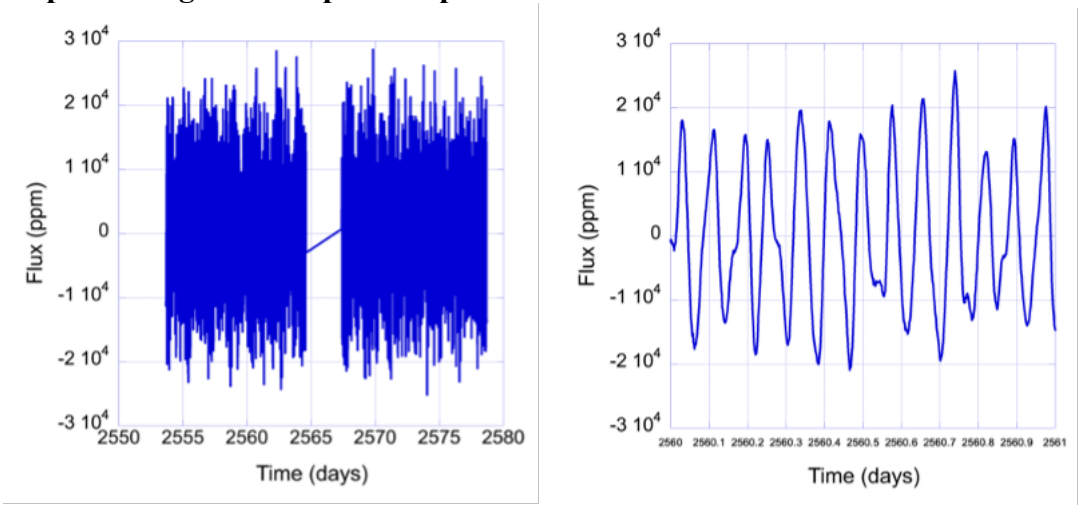

Figure 3. Left: FG Vir *TESS* 2-min cadence light curve from sector 46, showing 22.84 days of data, excluding the ~5-day gap in the middle of the data set. Time is measured after barycentric Julian day 2457000. Right: 1-day zoom-in on FG Vir *TESS* 2-min cadence data. Small features are resolved that were not resolved using *K2* 30-min cadence data.

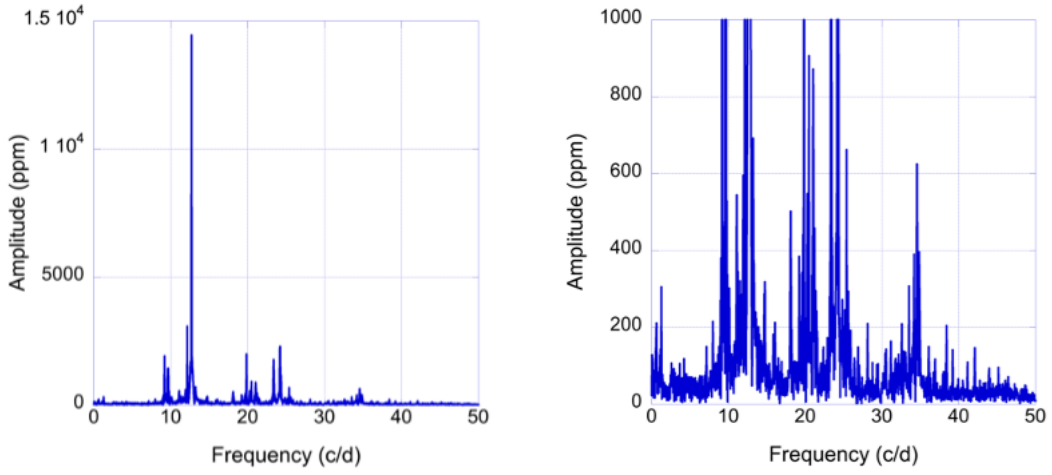

Figure 4. Left: FG Vir amplitude spectrum from *TESS* 2-min cadence data. Right: Zoom-in on low-amplitude portion of amplitude spectrum.

Table 1. FG Vir *K2* frequencies in order of S/N compared with Breger et al. (2005) frequencies. Low frequencies < 5 c/d are highlighted using red font.

Freq. #	Freq. (c/d)	Ampl. (ppt)	S/N	Combina-tions	Breger et al. Freq. (c/d)	Breger et al. Freq. #	Breger et al. S/N
f1	12.71762	14.671	140.862		12.7162	f1	442
f2	12.70894	2.593	24.857				
f3	12.15361	2.816	24.760		12.1541	f2	85
f4	9.65463	2.374	23.640		9.6563	f5	71
f5	9.19764	2.049	18.127		9.1991	f7	53
f6	24.22624	1.830	16.274		24.2280	f3	74
f7	23.40482	1.662	14.776		23.4034	f4	71
f8	24.19443	1.389	12.339		24.1940	f10	29
f9	12.72919	1.086	11.526				
f10	21.05045	1.185	10.405		21.0515	f6	55
f11	19.86748	0.968	8.610		19.8679	f8	55
f12	4.07820	0.850	8.285	*K2* thruster frequency			
f13	20.51248	0.810	7.052		20.5112	f35	6.6
f14	0.06942	0.775	6.883	8x (f1-f2) 6x (f9-f1)			
f15	20.28687	0.635	5.791		20.2878	f11	26
f16	12.79282	0.577	5.445		12.7944	f17	13
f17	0.31527	0.565	5.198				
f18	0.02603	0.610	5.162	3x (f1-f2)			
f19	19.22828	0.572	5.126		19.2278	f9	30
f20	4.09555	0.554	4.929	1f7-2f4			
f21	11.10369	0.562	4.926		11.1034	f20	11
f22	9.66331	0.511	4.613				
f23	0.63921	0.519	4.584				
f24	12.69448	0.513	4.550				
f25	0.52930	0.519	4.376				
f26	0.09834	0.440	4.243	3x (f9-f1)			
f27	23.50894	0.465	4.179				
f28	11.21071	0.481	4.111		11.2098	f38	6.4

f29	14.36915	0.463	4.070		34.5737*	f23	9.3
f30	14.73647	0.412	3.701		14.7354	f49	5.3
f31	1.91184	0.391	3.695				
f32	13.23535	0.408	3.640		13.2365	f27	8.3
f33	8.15640	0.410	3.596	2x *K2* thruster frequency			
f34	1.28998	0.408	3.542				
f35	0.49459	0.430	3.541	f9 - 3x *K2* thruster frequency			
f36	1.12512	0.393	3.479				
f37	0.67392	0.450	3.453				
f38	24.34772	0.378	3.368		24.3485	f18	12
f39	0.47434	0.368	3.280	f2 - 3x *K2* thruster frequency			
f40	1.99861	0.365	3.252				
f41	21.23267	0.360	3.229		21.2323	f16	14
f42	1.14537	0.362	3.037				
f43	1.03257	0.350	3.030				
f44	3.06010	0.353	3.009				
f45	2.95019	0.336	3.007				
f46	0.61896	0.330	2.949				

*Frequency reflected around Nyquist frequency of 24.4695 c/d

Table 2. 100 highest S/N FG Vir *TESS* frequencies. Low frequencies < 5 c/d are highlighted using red font.

Freq. #	Freq. (c/d)	Amplitude (ppt)	S/N	Combinations and Notes	Breger et al. (2005) Freq. #
f1	12.7151	13.828	3103.77	-	f1
f2	24.2147	2.687	663.11	-	f3
f3	12.1553	2.473	577.08	-	f2
f4	9.6523	2.133	516.96	-	f5
f5	23.4070	2.040	472.71	-	f4
f6	19.8644	1.879	427.32	-	f8
f7	9.1965	1.640	405.22	-	f7
f8	21.0479	1.461	296.56	-	f6

f9	24.1827	1.168	245.17	-	f10
f10	20.5121	0.799	184.54	-	f35
f11	34.5708	0.774	171.33	-	f23
f12	12.6911	0.681	171.30	close to f1	
f13	20.2882	0.703	167.20	-	f11
f14	25.4303	0.641	155.96	2f1	f15=2f1
f15	24.2547	0.703	150.47	close to f2	
f16	18.1291	0.630	139.94	-	
f17	34.8826	0.571	138.88	-	
f18	11.0998	0.551	130.22	-	f20
f19	14.7384	0.532	122.38	-	f49
f20	11.2117	0.547	121.35	-	f38
f21	24.3587	0.578	121.11	-	
f22	13.2349	0.483	111.78	-	f27
f23	9.6763	0.346	106.01	close to f4	
f24	21.2319	0.449	105.60	-	f16
f25	23.4390	0.396	100.50	-	f24
f26	19.6485	0.395	96.10	-	f65
f27	12.7951	0.401	89.56	-	f17
f28	34.1949	0.407	86.40	6f1-2f8	
f29	19.2246	0.351	80.59	-	f9
f30	19.8964	0.372	77.54	-	
f31	20.8320	0.330	75.00	-	f39
f32	11.9394	0.344	74.11	-	f29
f33	33.5312	0.325	73.59	-	
f34	1.2875	0.311	72.23	low frequency	
f35	9.2205	0.300	66.57	close to f7	
f36	24.8705	0.266	66.34	f1+f3	f1+f2
f37	25.6302	0.265	58.20	-	f68
f38	21.0239	0.249	58.05	close to f8	
f39	16.0738	0.257	57.53	-	f13
f40	23.4790	0.240	57.21	-	
f41	21.3998	0.259	55.73	2f17-2f9	
f42	19.3286	0.237	54.38	-	f41
f43	24.2867	0.193	53.63	-	
f44	25.1824	0.229	51.28	-	f30

f45	38.4173	0.220	50.73	f16+f13	
f46	28.1412	0.218	50.44	-	f19
f47	12.6112	0.184	50.16	-	
f48	11.6116	0.232	49.89	-	f50
f49	24.1507	0.217	49.02	2f9-f2	
f50	12.1234	0.223	48.74	close to f3	
f51	0.5038	0.208	47.94	low frequency	
f52	13.4429	0.211	47.00	-	
f53	34.1229	0.199	46.20	-	
f54	7.9889	0.194	44.92	-	f44
f55	10.1721	0.200	44.35	2f17-3f6	f25
f56	23.3750	0.197	42.44	-	
f57	9.6203	0.184	42.38	3f15-3f8	
f58	34.7627	0.181	42.25	-	
f59	12.7551	0.185	41.94	-	
f60	12.2353	0.177	40.80	-	
f61	24.5426	0.178	40.56	-	
f62	22.3754	0.176	40.41	-	f42=f1+f5
f63	32.5795	0.170	40.09	f1+f6	
f64	18.1610	0.166	38.52	-	
f65	31.2040	0.160	37.24	-	f57
f66	36.1222	0.162	37.11	f1+f5	f40=f1+f4
f67	33.9950	0.161	36.82	-	
f68	23.9988	0.214	36.54	-	f58
f69	11.7875	0.172	36.45	-	
f70	21.5677	0.153	35.86	-	
f71	21.4718	0.160	35.70	-	
f72	30.4603	0.155	34.95	-	
f73	23.8069	0.144	34.74	-	f48
f74	0.5918	0.152	34.66	low frequency	
f75	39.2170	0.150	33.82	-	f69
f76	25.4622	0.136	33.46	-	
f77	11.7075	0.150	33.36	-	f33
f78	31.7718	0.140	33.29	-	
f79	20.6721	0.148	32.70	-	
f80	11.4916	0.143	32.51	-	

f81	30.5483	0.143	32.35	2f7+f3	
f82	2.6630	0.142	32.34	low frequency	
f83	32.1797	0.139	31.86	-	
f84	32.8594	0.139	31.64	-	
f85	34.6587	0.141	31.62	2f5-f3	
f86	19.9763	0.149	31.02	2f10-f8	
f87	18.6009	0.141	30.99	-	
f88	25.9421	0.129	30.53	-	
f89	42.1039	0.133	30.51	-	f66
f90	15.8659	0.134	30.15	-	
f91	25.3903	0.132	30.10	-	
f92	26.9177	0.126	28.96	-	
f93	33.0433	0.126	28.59	-	f74
f94	20.1363	0.125	28.45	-	
f95	7.1493	0.124	28.39	f6-f1	
f96	14.5464	0.123	28.21	-	
f97	29.4927	0.123	28.14	f18+2f7	
f98	41.1922	0.123	27.99	-	
f99	17.8252	0.122	27.75	-	
f100	8.9006	0.119	27.19	2f17-3f13	

Table 3. Unstable low-degree frequencies of 1.82 $M_\odot$ FG Vir model.

Mode degree	Freq. (c/d)	Linear growth rate per period	Notes
0	12.1557	2.87E-06	radial fundamental mode
0	15.7240	3.30E-05	
0	19.4744	1.66E-04	
0	23.2361	5.67E-04	
0	27.0256	1.54E-03	
0	30.8235	3.32E-03	
0	34.6365	4.67E-03	
0	38.5319	3.27E-03	
1	9.4303	5.92E-09	
1	12.4568	3.87E-06	Nearest frequency to highest-

			amplitude observed mode
1	16.1672	4.23E-05	
1	19.6468	9.23E-05	
1	20.7309	1.61E-04	
1	24.3940	8.35E-04	
1	28.4415	2.24E-03	
1	32.3942	4.19E-03	
1	36.3191	4.57E-03	
1	40.3270	1.55E-03	
2	10.0989	5.41E-08	
2	11.8952	6.09E-07	
2	12.5352	1.72E-06	
2	14.3243	8.09E-06	
2	16.7172	3.68E-05	
2	19.3467	1.17E-04	
2	22.5367	4.33E-04	
2	26.3052	1.32E-03	
2	30.2200	3.06E-03	
2	32.6560	2.60E-04	
2	34.2273	4.55E-03	
2	38.1374	3.61E-03	
3	8.8390	4.69E-09	
3	9.7564	2.42E-09	
3	10.5646	1.52E-07	
3	11.9282	1.25E-06	
3	13.9073	3.88E-06	
3	15.5789	2.23E-05	
3	16.8010	2.97E-06	
3	18.7368	7.41E-05	
3	20.2535	1.23E-04	
3	23.6239	6.51E-04	
3	27.6333	1.87E-03	
3	31.6207	3.86E-03	
3	35.5724	4.76E-03	
3	39.4859	1.51E-03	
3	39.7631	8.63E-04	

393